Interesting Correlation Between Structure, Physicomechanical, Swelling and Sustained Transdermal Release Behavior of Diltiazem Hydrochloride in Various Poly(vinyl alcohol) Hydrogel Membranes

Tridib Bhunia,[1] Manas Bhowmik,[2] Dipankar Chattopadhyay,[1] Abhijit Bandyopadhyay[1]

[1]*Department of Polymer Science and Technology, University of Calcutta, Calcutta 700009, India*
[2]*Department of Pharmaceutical Technology, Jadavpur University, Calcutta 700032, India*

Received 31 July 2010; accepted 13 April 2011
DOI 10.1002/app.34678
Published online 5 January 2012 in Wiley Online Library (wileyonlinelibrary.com).

ABSTRACT: Interesting correlation between physicomechanical and *in vitro* release behavior of diltiazem hydrochloride has been obtained in physically treated poly(vinyl alcohol) (PVA) membranes of widely different molecular weights. Physical treatment could not raise crystallinity in dry state, but some of them show significant postswelled crystallinity and achieves elastomeric character. They also retain lot of equilibrium water, ideally suited for drug-impregnated transdermal patches. In effect, low molecular weight PVA and dimethyl sulfoxide-modified high molecular weight PVA membranes have shown acceptable release of diltiazem hydrochloride when compared with thermally treated high molecular weight PVA membrane. © 2012 Wiley Periodicals, Inc. J Appl Polym Sci 124: E177–E189, 2012

Key words: poly(vinyl alcohol); hydrogel; freeze-thaw; *in vitro*; controlled release

INTRODUCTION

Poly(vinyl alcohol) (PVA) is a versatile polymer with lot of commercial value.[1] It has different grades subject to different degree of hydrolysis from its precursor poly(vinyl acetate).[1] Extent of water absorption controls its crystallinity—higher water absorption generally leads to lower crystallinity and vice versa.[2] PVA is an excellent biocompatible and biodegradable polymer,[3] but its degree varies with the extent of hydrolysis and molecular weight. It forms strong hydrogel owing to extensive intramolecular and intermolecular hydrogen bonding with water.[4,5] The water uptake property of PVA, that is, its swelling behavior can be modulated either by passive networking, that is, physically by annealing or chemical crosslinking using bifunctional crosslinkers, such as dianhydrides,[6] diisocyanates,[7] glutaraldehydes,[8,9] and so on, and boric acid,[10] which simultaneously reacts with multiple hydroxyl groups of PVA. Network density, in both cases, governs the swelling behavior. Recently, hydrogels have been extensively studied as potential agent in numerous biomedical applications such as biosensors, bioreactors, bioseparators, tissue engineering, and drug delivery.[11–13] Some of the mostly studied polymers, include PVA, poly(acrylic acid), poly(methacrylic acid), poly (hydroxyethyl methacrylate), poly(acrylamide)-their blends/derivatives, and so on, and cellulosics (methyl cellulose, ethyl cellulose, etc.).

Potency of polymer hydrogels in advanced/controlled drug delivery application has been widely explored off late since conventional drug therapy (oral and intravenous) has a serious drawback of short therapeutic time forcing into multiple administrations and drug overload problems in the body. The only advantage of conventional therapy is its low cost. Polymer hydrogel membranes/films encapsulate biomolecules such as water soluble proteins and drugs on account of their high viscosity and attractive interaction with the matrix and provide a resistive pathway against its outward diffusion. Thus, the elution of drug/biomolecules from hydrogels could be controlled, which finally leads to wider therapeutic window. Kim et al.,[14] in a recent literature, has demonstrated time profile of the actions of differently administered drugs in the body. They have also provided a list of various polymeric gels explored *in vivo* and *in vitro* for controlled release studies.[14] *In vivo* application is more targeted organ specific and is termed as "targeted drug delivery/on-site release" as these gels attains three-

Correspondence to: A. Bandyopadhyay (abpoly@caluniv.ac.in).

Contract grant sponsor: Council of Scientific and Industrial Research, Govt. of India.

dimensional structures to slow down the release under the influence of the ambience at the targeted sites (sensors). Externally applied gels usually do not have to meet this stringent criterion but should possess the property of steady transdermal release directly to the blood at body temperature. This is presently coined as "patch therapy" approach in latest medical science.

The use of PVA hydrogel either solely or in combination with other natural/synthetic polymers, that is, modified PVA, in advanced/controlled drug delivery has been reported in last 5 years.[15–17] Freezing–melting operation on PVA is a traditional approach to improve its crystallinity, and literatures are abundant on this subject.[18–21] The effect of freeze-thaw variables on different physicomechanical properties of PVA has been discussed in most of these literatures with little mention about the effect of varying PVA molecular weights. Further, almost none of these reports project these hydrogels as potential matrix for sustained drug delivery application. To illustrate a few, Lozinsky et al.[22] have experimented with PVA hydrogels of molecular weights 69 and 86 KDa but did not refer to drug release studies using these hydrogels. Likewise, few literatures report,[23–25] poly(ethylene glycol) (PEG) and dimethyl sulfoxide (DMSO) modification of PVA hydrogels but have not discussed transdermal release of diltiazem hydrochloride or similar kind of drugs. Diltiazem is water soluble, calcium channel blocker antianginal drug and is often used in the treatment of angina pectoris (chest pain). It functions by reducing the oxygen demand of the heart. Minimum required dose for an adult individual is 180 mg/day and is marketed as 30, 60, 90, and 120 mg tablets. It requires multiple oral in take on demand. Nonetheless, oral administration takes minimum 30 min to release the drug into the blood for therapeutic action. As an alternative measure, we have loaded this drug in thermally treated PVA membranes of widely different molecular weights and monitored its transdermal release directly to the blood through a model experiment. Some more experiments with PEG- and DMSO-modified high molecular weight PVA hydrogels have been conducted to see the variation. The results obtained have been correlated to various microstructures of respective hydrogels.

EXPERIMENTAL

Materials

PVA of two different number average molecular weights namely 1.15×10^5 (designated as PVA_H) and 1.4×10^4 (designated as PVA_L) have been used for this study. Both these semicrystalline polymers are high hydrolyzed grade (98%) and were purchased from E-Merck, Mumbai, India. PEG of two different molecular weights, 200 and 6000, and DMSO were added into high molecular weight PVA as modifiers. PEG was procured from Loba Chem, Mumbai, India, and DMSO (density 1100 Kg/m^3) of standard laboratory grade was obtained from indigenous source. The drug, diltiazem hydrochloride (molecular weight 450.98) was generously supplied by Ranbaxy Laboratories, Gurgoan, Haryana, India.

Preparation of hydrogel membranes

All PVA hydrogels were prepared by dissolving PVA in distilled water. PVA_H was soluble in boiling water whereas PVA_L was dissolved at room temperature. PVA solutions of 15/20 w/v% were prepared for analysis. After homogeneous mixing, aqueous PVA sol was cast into thin films on Teflon sheet for spontaneous air drying at room temperature. Samples with PEG was prepared by adding 10% aqueous PEG with respect to PVA_H. PVA_H with DMSO was prepared by replacing 50% of water by DMSO, and the membranes were obtained following similar procedure. Room temperature dried hydrogel membranes were then subjected to freezing at $-20^\circ C$ followed by thawing at $+50^\circ C$ for variable time periods. Details of all the samples are reported in Table I. Optimization of treatment temperature was based on mechanical property study. The average thickness of PVA films/membranes was maintained at 0.25 cm.

Analysis of hydrogels

Fourier transform infrared spectroscopic study

At room temperature ($27 \pm 2^\circ C$), Fourier transform infrared (FTIR) spectroscopic analysis of all the hydrogel membranes was done in a JASCO FTIR machine within the spectral range of 400–4000 cm^{-1} using a resolution of 4 cm^{-1} in dispersive mode. An average of 120 scans for each sample was reported for analysis.

X-ray diffraction studies

Wide angle (X-ray diffraction) XRD analysis of the hydrogel membranes was done in a X'pert PRO MRD X-ray diffractometer (PANalytical, The Netherlands) at room temperature ($27 \pm 2^\circ C$). The hydrogels were scanned in-between angles 10 and 40°. Spectral data corresponding to both dry and wet hydrogels were collected and are represented for analysis.

Microscopic studies

Polarized light microscopy

Optical microscopic images of the hydrogels were taken in a polarized light microscope (PLM), Leitz,

TABLE I
Hydrogel Sample Composition, Diffusion Exponents and Respective t_{50} Values

Sample designation	PVA (w/v)	F/T[I] Time cycle (h)	PEG_{200}[II] PEG_{6000}	DMSO[III]	n	m[IV]	t_{50} (hr)
PVA_H	20	0			0.239		
$PVA_{H/20/5/1c}$	20	5h1c			0.360	0.9898	393
$PVA_{H/15/5/1c}$	15	5h1c			0.335		
$PVA_{H/20/1/5c}$	20	1h5c			0.275		
$PVA_{H/20/3/1c}$	20	3h1c			0.330		
$PVA_{H/20/1/1c}$	20	1h1c			0.235		
$PVA_{H/20/5/1c/PEG6000}$	20	5h1c	10 wt% of PVA		0.382		
$PVA_{H/20/5/1c/PEG200}$	20	5h1c	10 wt% of PVA		0.256		
$PVA_{H/20/5/1c/DMSO}$	20	5h1c		1 : 1 water : DMSO as PVA solvent	0.070	0.7438	145
PVA_L	20	0			0.362		
$PVA_{L/20/5/1c}$	20	5h1c			0.563	0.7049	113
$PVA_{L/20/1/5c}$	20	1h5c			0.250		
$PVA_{L/20/3/1c}$	20	3h1c			0.277		

[I] Freezing- thawing cycle time.
[II] PEG_{6000}-PEG of molecular weight 6000 and PEG_{200}-PEG of molecular weight 200.
[III] 50% of total water has been replaced by DMSO.
[IV] m value (drug exponent) for drug release process.

Germany, using a uniform magnification of ×100. Continuous pictures of the PVA hydrogels during heating were captured by placing hydrogel membranes over a electrically heated glass slide (heating rate 10°C min^{-1}).

Atomic force microscopy

Morphology study of the hydrogels were carried out in air at 27 ± 2°C utilizing multimode atomic force microscopy (AFM) from VEECO Digital Instruments, Santa Barbara, CA. Topographic phase images were recorded in taping mode (TMAFM) with set point ratio of 0.9 using rotated tapping etched silicon probe tip having spring constant of 40 N m^{-1}. The cantilever was oscillated at a resonance frequency of 280 KHz.

Mechanical properties study

Tensile stress–strain properties (tensile strength, modulus, and elongation-at-break) of the dry and fully swollen hydrogels were studied in a Lloyd UTM, UK. All the experiments were carried out at room temperature (27 ± 2°C), with hydrogel membranes cut as per dimension of ASTM Die C, and were pulled at a rate of 10 mm min^{-1}. An average of five test results has been reported for analysis.

Swelling and deswelling kinetics study

Swelling of hydrogel membranes was done after putting membranes of uniform dimension (5 × 2 × 0.25 cm^3) in distilled water at room temperature (27 ± 2°C). After stipulated time interval, the samples were taken out of the water, gently wiped in tissue paper to soak surface water and then weighed in an electronic balance. The swelling ratio was calculated by dividing swelled weight (S) by dry weight (S_0) of the hydrogel. The experiment was carried out till the samples attained equilibrium. Care was taken to avoid partial sample loss due to dissolution.

Deswelling experiment was done by periodically recording the decreasing weight of the fully swollen gel films in ambient air (27°C, RH: 85) till constant value.

Drug release kinetics study

In vitro drug release kinetics study using selective hydrogel membranes were performed by using a Franz diffusion cell (Scheme 1) after loading the drug into the membrane. The drug (1 mg) was mixed thoroughly with PVA sol for 1 h at room temperature, cast on plane Teflon sheet, and freeze-thawed using similar procedure. A dialysis membrane (LA390, average flat width 25.27 mm, average diameter 15.9 mm, and capacity ~ 1.99 mL cm^{-1}) made from cellulose acetate was used as human skin replica.[26] The membrane was mounted between the donor and receptor compartments of the diffusion cell.[27] The hydrogel membrane was placed over that and covered with an aluminum foil. The receptor compartment was filled with phosphate buffer of pH 5.6 to match the skin pH (5.4–6.9).[28] The whole assembly was fixed on a hot-plate magnetic stirrer, and the solution in the receptor compartment was continuously stirred using magnetic beads to maintain a steady temperature at 32 ± 0.5°C, exactly same to normal human skin temperature 32°C.[29] The

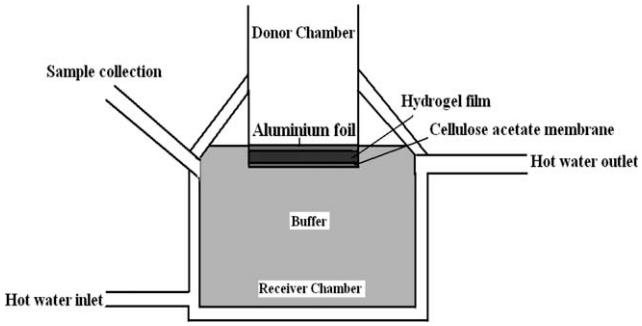

Scheme 1 Franz diffusion cell.

aliquots were withdrawn at different time intervals and were replenished with an equal volume of fresh buffer. The diltiazem hydrochloride content in the aliquots was analyzed spectrophotometrically at 236 nm after matching the values with a standard calibration plot.

RESULTS AND DISCUSSION

Fourier transform infrared spectroscopic analysis of the hydrogels

Figure 1(a) shows the FTIR spectrum of neat, solvent cast PVA_H membrane. All the characteristic peaks are explained in the figure itself. Spectrum of $PVA_{H/20/5/1c}$ has been stacked along with neat PVA_H to show differences due to annealing. By and large, greater peak/band resolution in $PVA_{H/20/5/1c}$ indicates rise in crystallinity after freeze-thaw treatment. Absorbance at 1140 cm^{-1} is of particular interest as it appears in crystalline form of PVA only. It is clearly seen in $PVA_{H/20/5/1c}$. Ratio of peak intensities at 1140 cm^{-1} to that of 850 cm^{-1} has been used as the relative measure of the extent of crystallinity[30] developed after freeze-thaw treatment. I_{850} (intensity) is used as an internal standard as it does not change during crystallization. Please note that solvent cast PVA_H is predominantly amorphous under experimental condition because it does not show any clear absorbance at 1140 cm^{-1} [Fig. 1(a)].

Figure 1(b,c) compares the intensity ratio (I_{1140}/I_{850}) in different PVA membranes taken from their normalized spectra (normalized against absorbance at 850 cm^{-1}). Literally, there is no rise in crystallinity in high molecular weight gels after annealing for 1 and 3 h, but, after 5 h, there is a steep rise in crystallinity. However, PVA_H membranes prepared with lower PVA concentration (15 wt %) than the standard 20 wt % does not exhibit such crystallization after 5 h freeze-thaw treatment [Fig. 1(b)]. Nevertheless, no significant rise in crystallinity is observed after the addition of low molecular weight PEG (molecular weight 200) but all of a sudden, high molecular weight PEG (molecular weight 6000) and DMSO-modified PVA_H have recorded tremendous rise in crystallinity after 5 h freezing–melting cycle. Conversely, the steady rise in crystallinity with increase in thermal treatment is observed with

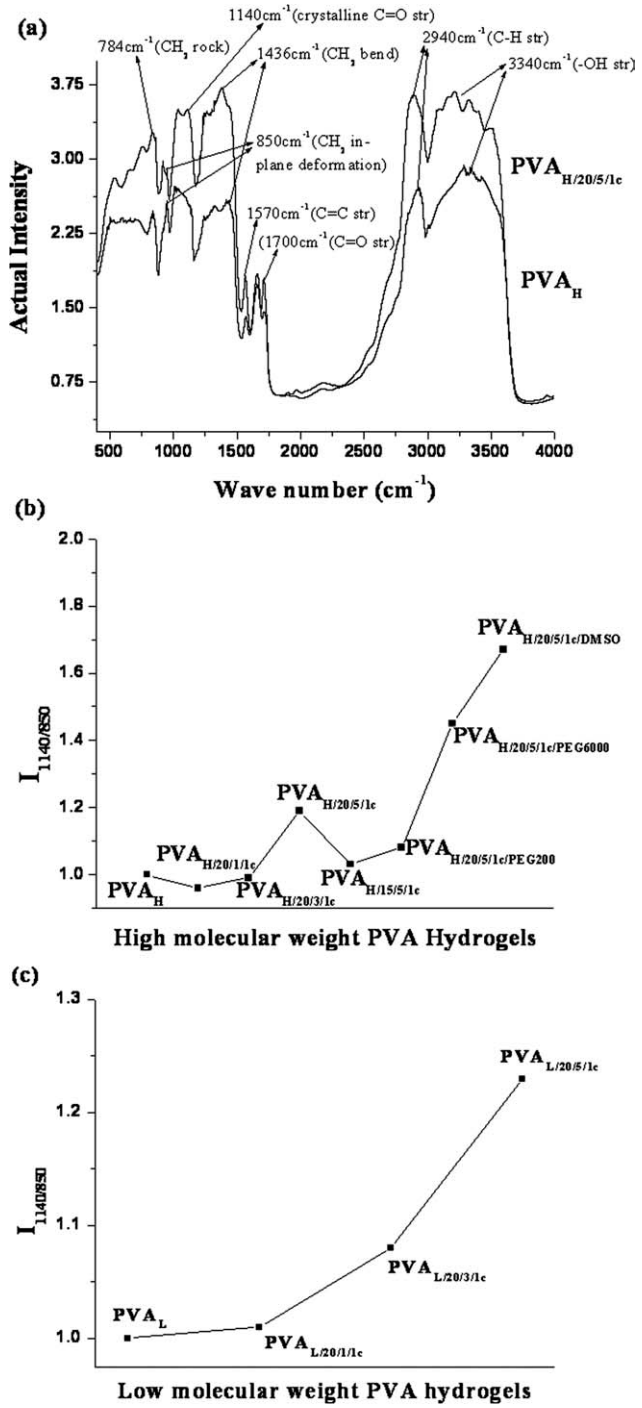

Figure 1 (a) FTIR spectra of solvent cast PVAH and PVAH/20/5/1c membranes. FTIR Peak intensity ratio (I(1140/850)) of (b) high and (c) low molecular weight PVA hydrogel membranes.

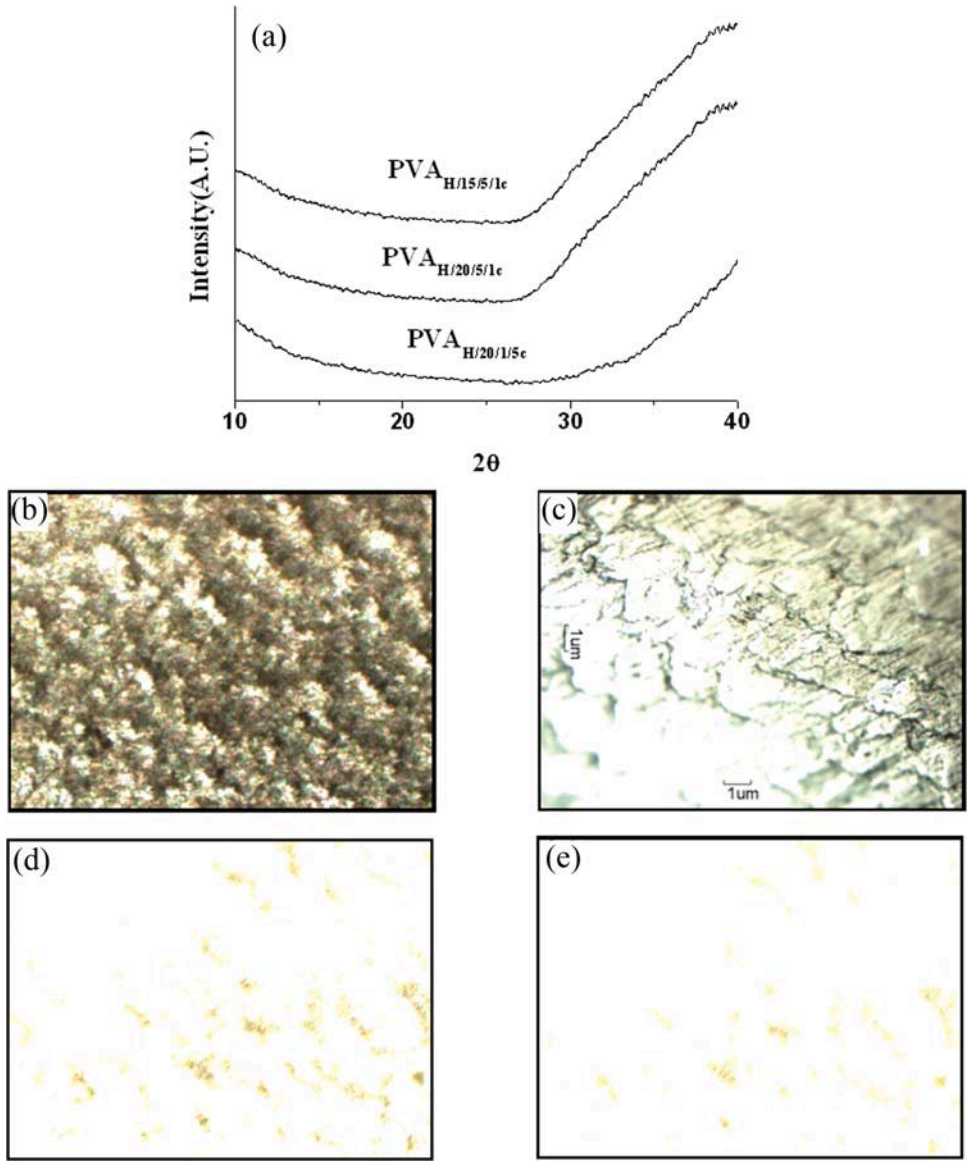

Figure 2 (a) X-ray diffractograms of high molecular weight PVA hydrogels and hot stage optical microscopic images of representative PVAH/20/5/1c at (b) initial, (c) after 2 min, (d) after 5 min, and (e) final stage of heating. XRD spectra of (f) PEG and DMSO modified PVAH hydrogels and (g) treated PVAL hydrogel in dry state. Spectra in (h), (i), and (j) corresponds to swelled PVAH, modified PVAH and thermally treated PVAL hydrogels respectively. [Color figure can be viewed in the online issue, which is available at wileyonlinelibrary.com.]

low molecular weight PVA hydrogels, shown in Figure 1(c).

X-ray diffraction analysis of the hydrogels

Figure 2(a,f–j) shows wide angle X-ray diffractograms of various PVA hydrogel membranes. The spectra have been taken both in preswelled and postswelled states of the gels. Dry PVA_H really do not show any diffraction peaks after thermal treatment [Fig. 2(a)]. Though, according to literature reports, crystallinity does appear in solvent cast high molecular weight PVA[19] and further increases on increasing freezing-thawing cycles.[21] Our results do not show any crystalline diffractions within its normal range ($2\theta = 18–20^\circ$) despite of the fact that FTIR peak intensity ratio had already given fair indication of rise in crystallinity in these hydrogels. Amorphous volume fraction probably dominates over crystalline volume fraction and leads to such contrasting observations. XRD technique detects volume percent crystallinity, which in this case remained undetected as the amorphous fraction predominates. However, it is efficiently detected via FTIR spectroscopy as it records microstructural changes in the matrix.

According to Florian,[31] there can be different states of water such as "free" and "bound" in the

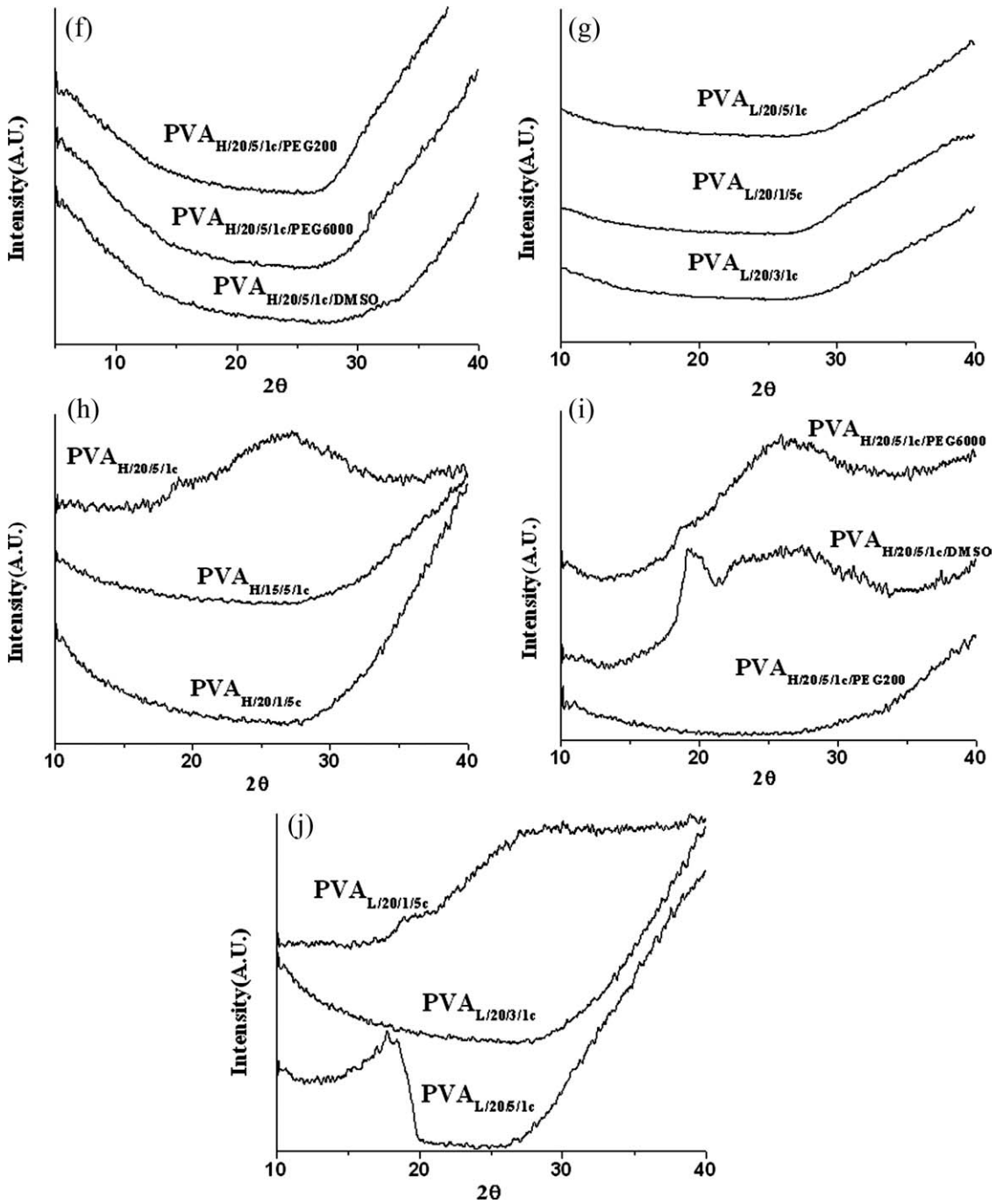

Figure 2 (*Continued*).

hydrogels. The relative proportion of these could vary depending on nature of the polymer and its hydrodynamic volume. It is also known that aqueous PVA gradually turns hazy on standing due to macrophase separation. On freezing, a portion of water in hydrogels form ice, may be called as "freezable-free water" and goes into crystalline phase, whereas the polymer (PVA) does not. On heating, ice melts and interacts with PVA reforming hydrogen bonds. PVA_H does have lower hydrodynamic volume mainly due to poor water solubility and high chain-entanglement density, and, thus, all PVA_H-water hydrogen bonds during thawing (heating) operation could not be restored. Increasing duration of freezing–melting cycles (from 3 to 5 h) and PVA concentration (15–20 wt %) leads to more phase separation as all of these hydrogels visually appeared "less" transparent after treatment. It was presumed that loss in transparency was due to "increase" in crystallinity as complementary to infrared spectroscopic observation but later on, XRD together with online monitoring of representative

$PVA_{H/20/5/1c}$ during heating under PLM identified these as "amorphous water-bound PVA microaggregates" after detecting prominent shrinkage of darker domains (due to the removal of bound water) on heating the gel up to 150°C under PLM (below melting point of PVA). The initial [Fig. 2(b)], final [Fig. 2(e)], and two intermittent PLM pictures [Fig. 2(c,d)] of this phenomenon are demonstrated as ready reference. Modification with low ($M_n = 200$) and high ($M_n = 6000$) molecular weight PEG and further by DMSO (better solvent than water) still could not raise volume percent crystallinity in PVA_H [Fig. 2(f)]. But one special observation in this set of samples is the physical feel of $PVA_{H/20/5/1c/DMSO}$. It appears completely leathery and was entirely different from all other samples possibly due to higher solubility of PVA in the mixed solvent (water-DMSO). PEG eventually increases number of available hydroxyl (OH) groups in the hydrogels but fails to induce any crystallinity due to increase in equilibrium moisture content than usual. Figure 2(g) shows XRD spectra of PVA_L hydrogels. Afresh, no clear crystalline peak is seen at $2\theta = 18$–$20°$ indicating the absence of any crystalline PVA domains in these hydrogels after 5 h of freezing-thawing operations. Nevertheless, the "amorphous halo" ranging from $2\theta = 30°$ to 40° together with higher intensity of the diffractograms compared to PVA_H [Fig. 2(a)] probably results from predominant water bound amorphous PVA phases inside gel matrix when compared with PVA_H. PVA_L due to its high hydrodynamic volume interacts strongly with "free" water phase in the gel through hydrogen bonding and results into "more compact" PVA-water macrostructure inside the gel matrix in the unswelled state.

XRD spectra of fully swollen hydrogels are shown in Figures 2(h–j). The changes are clearly visible especially for modified PVA_H and thermally treated PVA_L hydrogels. On "external" water uptake, a diffused diffraction peak at $2\theta = 18°$ appears in $PVA_{H/20/5/1c}$ along with strong PVA-water hydrogen-bonded broad peak at $2\theta = 27°$ [Fig. 2(h)]. $PVA_{H/20/1/5c}$ does not show similar peaks but shows significant increase in diffraction intensity of the amorphous region [Fig. 2(h)]. However, $PVA_{H/15/5/1c}$ does not show any detectable morphological differences between swelled and unswelled states. Diffraction peak at $2\theta = 18$–$20°$ is more clear and distinct in DMSO and high molecular weight PEG-modified PVA_H hydrogels (former has shown stronger diffraction) and also in PVA_L gels displayed in Figure 2(i,j), while, there is no such changes observed in $PVA_{H/20/5/1c/PEG200}$. $PVA_{H/20/5/1c/PEG6000}$ has shown a small peak at $2\theta = 18°$ which is then merged with the subsequent water-bound PVA amorphous halo. In $PVA_{H/20/5/1c/DMSO}$, the PVA diffraction peak at $2\theta = 18°$ is the strongest among all the swollen samples; there is another very fine peak at $2\theta = 20°$. Beyond this, there is a large amorphous domain of water bound PVA phase. In PVA_L hydrogels, prominent PVA diffraction peaks are observed in $PVA_{L/20/5/1c}$ while slightly diffused and merger type in $PVA_{L/20/1/5c.}$ Crystallinity appearing after equilibrium swelling in some of these hydrogels is surely a new observation for future references. This probably results due to dissolution of amorphous domains on swelling leading to rise in volume percent crystallinity, which, although weakly, is now detectable through XRD. It is to be noted that, these particular samples have swelled slowly than those, where nocrystallinity has been recorded at postswelled stage. This further compliments our earlier assumption on predominant amorphous character of these hydrogels in the dry state.

Morphological investigation through atomic force microscopy and polarized light microscopy

Figure 3(a,b) shows AFM phase images of representative PVA_H and PVA_L hydrogels taken in the postswelled state. White domains are hard crystalline domains while gray portions are soft, amorphous regions. Transit phases are of intermediate color in the swollen gels. Volume concentration of hard crystalline domains in $PVA_{L/20/5/1c}$ [Fig. 3(b)] is clearly much higher when compared with $PVA_{H/20/5/1c}$ [Fig. 3(a)], excellently complementing our postswelled XRD data. This, on larger scale, is visualized through PLM images of the samples where crystalline domains appear opaque as the light gets obstructed [Fig. 3(c–e)]. Opacity is much lighter in $PVA_{H/20/5/1c}$ [Fig. 3(c)] whereas significantly higher in $PVA_{L/20/5/1c}$ [Fig. 3(d)] and $PVA_{L/20/5/1c/DMSO}$ [Fig. 3(e)] in the postswelled state.

Studies on mechanical properties of the hydrogels

Figure 4 demonstrates tensile properties of various PVA hydrogels determined before and after equilibrium swelling experiments. It is well established that mechanical properties of PVA strongly depends on its moisture sensitivity. Moisture absorption, however, is a function of its physicochemical structure. Figure 4(a) shows the mechanical properties of dry PVA_H membranes and similar properties of PEG- and DMSO-modified PVA_H membranes are displayed in Figure 4(b). DMSO-modified hydrogel was "leathery," and it shows lowest modulus and tensile strength amid all the samples. Untreated/unmodified PVA_H has shown slightly higher strength than $PVA_{H/20/5/1c/DMSO}$ but is convincingly lower than remaining all other hydrogels in this series; the elongation at failure is 100% for this (PVA_H) as compared with almost 200% for rest of the membranes

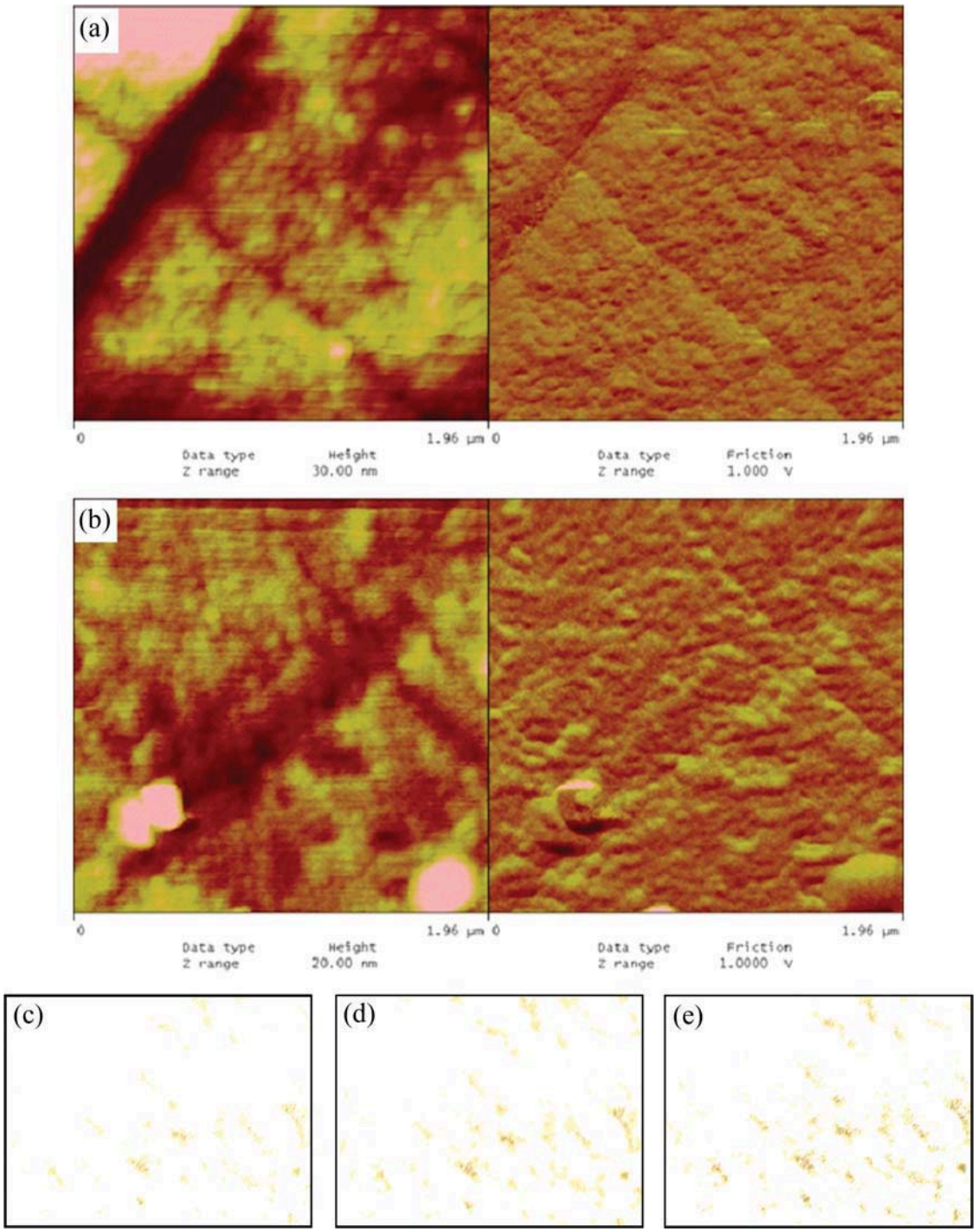

Figure 3 AFM phase images of (a) PVAH/20/5/1c and (b) PVAL/20/5/1c after equilibrium swelling. Postswelled optical microscopic images of (c) PVAH/20/5/1c, (d) PVAL/20/5/1c, and (e) PVAL/20/5/1c/DMSO hybrid hydrogel membranes. [Color figure can be viewed in the online issue, which is available at wileyonlinelibrary.com.]

barring $PVA_{H/20/5/1c/PEG6000}$. Tensile modulus and ultimate tensile strength gradually increase on increasing freeze-thaw treatment time (3 and 5 h) and PVA concentration. PEG 6000 modified hydrogel has recorded maximum tensile strength and modulus values, whereas the gel modified with low molecular weight PEG has shown much lower values of similar properties. Rise in tensile strength reflects rise in bulk crystallinity, which oddly has been reflected through FTIR spectroscopy. Addition of high molecular weight PEG increases net weight of the high molecular weight components in the gel and, hence, the gel has recorded highest mechanical properties. With low molecular weight PEG, the reverse has happened. Figure 4(c) displays tensile stress–strain properties of PVA_L hydrogels. As low

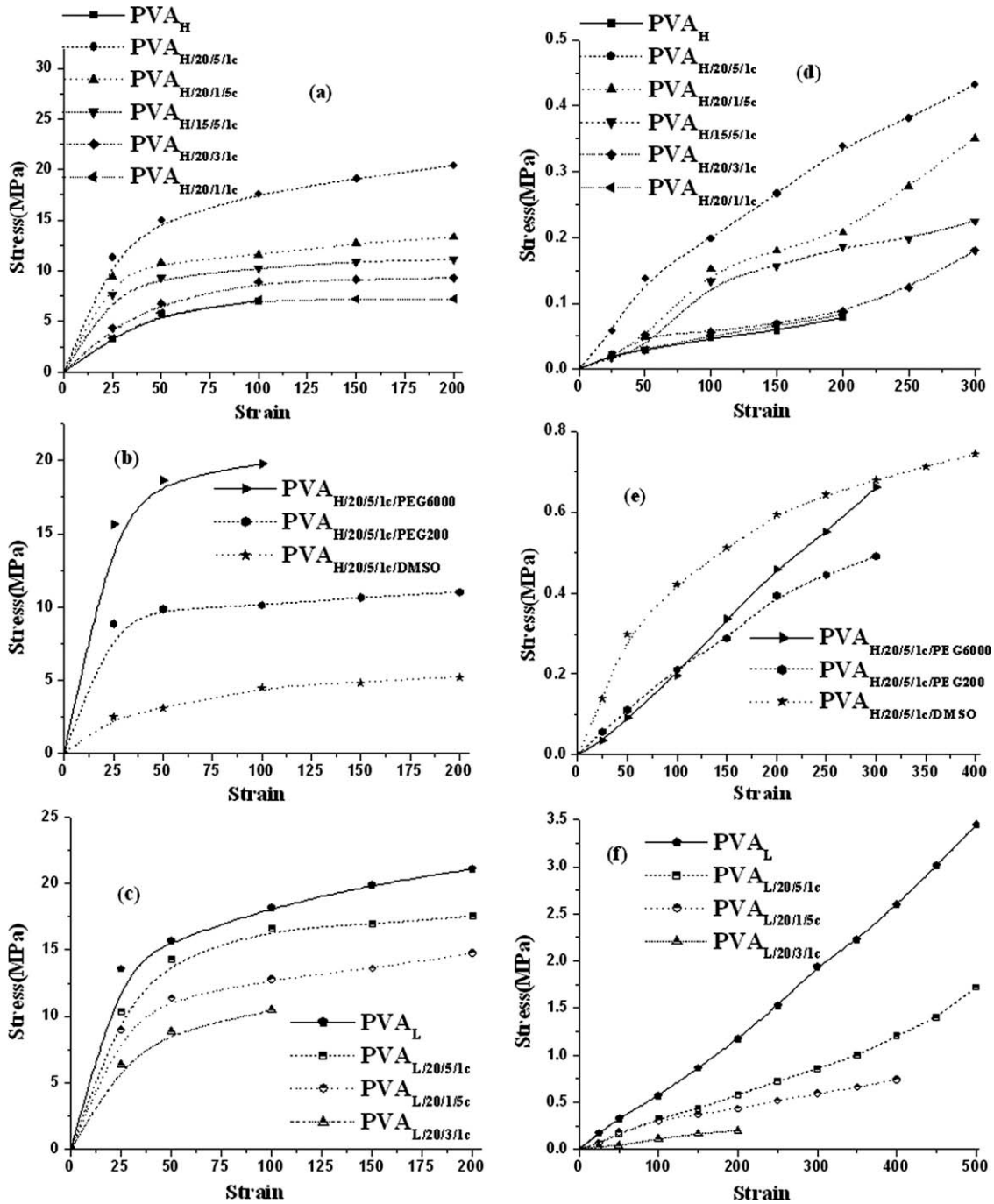

Figure 4 Mechanical properties study of (a) treated PVAH (b) PEG and DMSO modified PVAH and (c) treated PVAL hydrogel membranes in dry state and (d), (e), and (f) represents similar studies on respective swelled hydrogels.

molecular weight samples are more water soluble, they have recorded higher mechanical properties (tensile modulus and ultimate tensile strength) after similar treatment due to stronger PVA-water interaction as already mentioned. Unlike PVA_H, PVA_L hydrogels show regular trend, that is, samples after higher freeze-thaw time registers higher strength [because of more crystalline PVA domains inside the gel matrix as per FTIR results in Fig. 1(c)]. Tensile behavior of all PVA_H and PVA_L gels, after equilibrium swelling, is shown in Figure 4(d–f). Overall, the strength has gone down and elongation at break values increase significantly, illustrating elastomeric nature after external water uptake. In fact, the swelling leads to few interesting observations. The "yield" behavior is not seen for most of these hydrogels indicating that these are "reinforced" through swelling action. Samples such as $PVA_{H/15/5/1c}$ and $PVA_{H/20/5/1c}$ have shown some nonlinear deformation behavior alike elastomers, due to chain-

unfolding mechanism. $PVA_{H/20/5/1c/DMSO}$ shows maximum modulus, strength, and elongation simultaneously, commensurating its high crystallinity in the swelled state. Low hydroxyl group concentration than ordinary PVA probably impart some plasticization effect by reducing hydrogen-bonded interaction and highly elongates the gel before complete failure. Hydrogels of low molecular weight PVA supersede its high molecular weight counterpart both in overall strength and elongation properties. $PVA_{L/20/5/1c}$ shows an ultimate tensile strength of 3.5 MPa and 500% elongation which is quite interesting. Similar trends are recorded for $PVA_{L/20/1/5c}$ and $PVA_{L/20/3/1c}$ too. These are ascribed to higher volume crystallinity in these gels than in its high molecular weight counterpart. Less PVA-water interaction (due to low molecular weight PVA) similar to $PVA_{H/20/5/1c/DMSO}$ especially at the amorphous domains inside the matrix, results in huge elongation principally due to plasticizing effect of water. The mechanical property data especially in postswelled state are significant in respect of drug delivery prospects. High matrix strength together with elastomeric nature offers an excellent combination of various physical properties in some of these hydrogels and creates lot of interests for their prospective use as diltiazem releaser.

Studies on swelling and deswelling behavior of the hydrogels

Figure 5 illustrates extensive swelling and deswelling properties of PVA hydrogels carried out under ambient condition. Swelling experiments are continued till equilibrium is reached. This is shown by broken time axis in the figures. Hydrogels devoid of any freeze-thaw treatment have shown maximum water uptake and also at maximum rate. Swelling of the gels has been more controlled after freeze-thaw operation; rate of swelling and net water uptake have decreased. These are shown in Figure 5(a). $PVA_{H/20/1/1c}$ and untreated PVA, both have shown similar behavior indicating the fact that almost no crystallization has occurred in the former after 1 h of freezing–melting treatment. Further rise in freeze-thaw treatment time reduces rate and extent of swelling, just mentioned. Only a slight difference in swelling behavior observed among $PVA_{H/20/5/1c}$, $PVA_{H/20/1/5c}$, $PVA_{H/15/5/1c}$, and $PVA_{H/20/5/1c/PEG6000}$ [Fig. 5(b)]. All these samples were predominantly amorphous and have swelled at an appreciable rate. $PVA_{H/20/5/1c/PEG6000}$ unlike others, has some additional OH groups to contribute in its swelling behavior. Samples such as $PVA_{H/20/5/1c/PEG200}$ and $PVA_{H/20/5/1c/DMSO}$ have shown much restricted swelling compared to others [later is most resistant as per Fig. 5(b)]. Swelling behavior of low molecular weight PVA hydrogels are shown in Figure 5(c). PVA_L without any freeze-thaw treatment has shown tremendous swelling when compared with rest of the compositions but when compared with its high molecular weight counterpart, it is still slower mainly due to its low OH group content [Fig. 5(a)]. Increase in freeze-thaw time has reduced the swelling rate considerably. The lowest has been observed with $PVA_{L/20/5/1c}$. Unlike PVA_H, there is fair amount of difference in rate and extent of swelling among $PVA_{L/20/5/1c}$ and $PVA_{L/20/1/5c}$ membranes possibly due to the reason that it becomes more crystalline on course of swelling. An attempt has been made to theorize swelling kinetics of these hydrogels through a mathematical model. By and large, the swelling behavior is fast at initial stage but after some time, it gradually slows down and finally equilibrates. Phenomenological rate expression [eq. (1)] is used to describe such swelling kinetics.

$$S/S_0 = kt^n \tag{1}$$

k is "swelling ratio front factor" and n is "swelling exponent." Swelling mechanism is described by the value of n obtained after straight-line fitting to double logarithmic plots of the parameters in eq. (1). The n values of different hydrogels are reported in Table I. Noticeably, all the hydrogels show $n < 0.5$. This means the transport mechanism of water is predominantly diffusion controlled (Fickian mechanism) in all these membranes and not through molecular relaxation of PVA chains (non-Fickian or anomalous mechanism).

Deswelling kinetics of these hydrogels is shown in Figure 5(d–f). Results on thermally treated PVA_H gels are displayed in Figure 5(d). Neat PVA_H and $PVA_{H/20/3/1c}$ have lost their equilibrium water at faster rate and finally could retain only smaller amount of water when compared with other samples in the series. $PVA_{H/15/5/1c}$ initially loses water at a faster rate but slows down soon and finally retains greater amount of equilibrium water than both PVA_H and $PVA_{H/20/3/1c}$, and also from PEG modified systems shown in Figure 5(e). Samples such as $PVA_{H/20/5/1c}$, $PVA_{H/20/1/5c}$, and $PVA_{H/20/5/1c/DMSO}$ [$PVA_{H/20/5/1c/DMSO}$ in Fig. 5(e)] have exhibited slow water loss behavior with time and also retains greater amount of equilibrium water than rest of the samples in the series. In PVA_L series, neat PVA, $PVA_{L/20/1/5c}$, and $PVA_{L/20/3/1c}$ have shown relatively faster deswelling rate with neat PVA being the fastest [Fig. 5(f)]. $PVA_{L/20/5/1c}$ shows slow release with time and also retains maximum amount of equilibrium water than any of the hydrogels in this series. Annealed hydrogels those treated for 5 h and particularly DMSO-modified samples have retained lot of water in comparison to other samples may be due to two reasons. First, the available free water for diffusion is low due to low swelling and

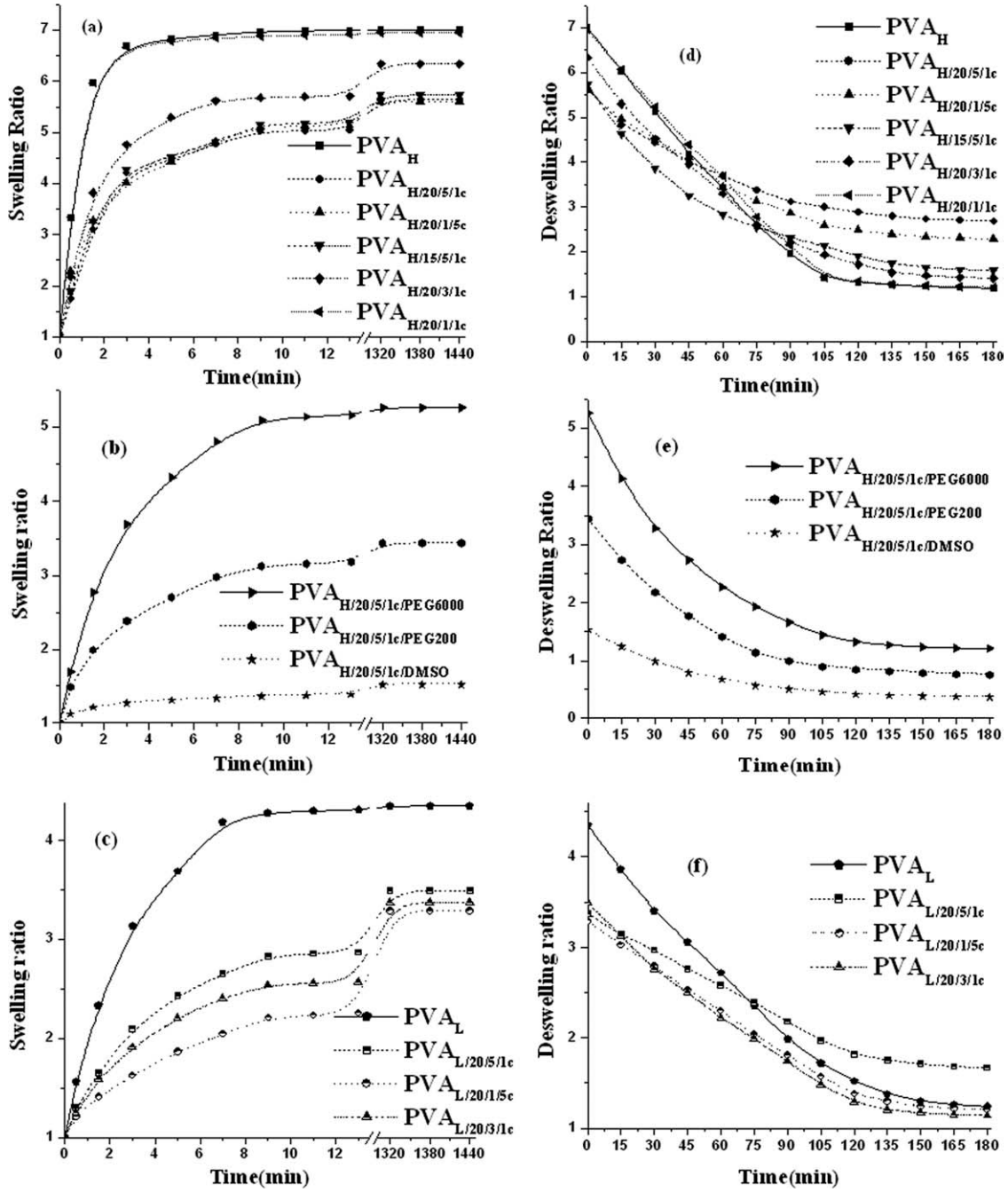

Figure 5 Swelling and deswelling kinetic investigation: Swelling studies of (a) treated PVAH, (b) PEG- and DMSO-modified PVAH, and (c) treated PVAL hydrogel membranes and (d), (e), and (f) represents deswelling behavior of the respective hydrogels.

second, the equilibrium water content in these hydrogels are primarily attached to crystalline domains and are, therefore, strongly retained. This is an important property of these hydrogel membranes in addition to their mechanical strength as they would not dry up fast and will retain lot of moisture to keep the underneath skin cool when applied for patch therapy.

In vitro transdermal release studies of diltiazem hydrochloride

The experimental detail of this study was described in the experimental section. Figure 6 compares the release kinetics of diltiazem hydrochloride through representative $PVA_{H/20/5/1c}$, $PVA_{H/20/5/1c/DMSO}$, and $PVA_{L/20/5/1c}$ hydrogel membranes as they have shown exciting physicomechanicals. A constant release study up to 12 h has been conducted, and the data points are reported (Fig. 6) along with respective t_{50} values in Table I. It is clear that the release of diltiazem hydrochloride is considerably slow and hence controlled. $PVA_{H/20/5/1c}$ has allowed only 1% release whereas $PVA_{L/20/5/1c}$ and $PVA_{H/20/5/1c/DMSO}$ have allowed about 5 and 6% cumulative release of the loaded drug, respectively.

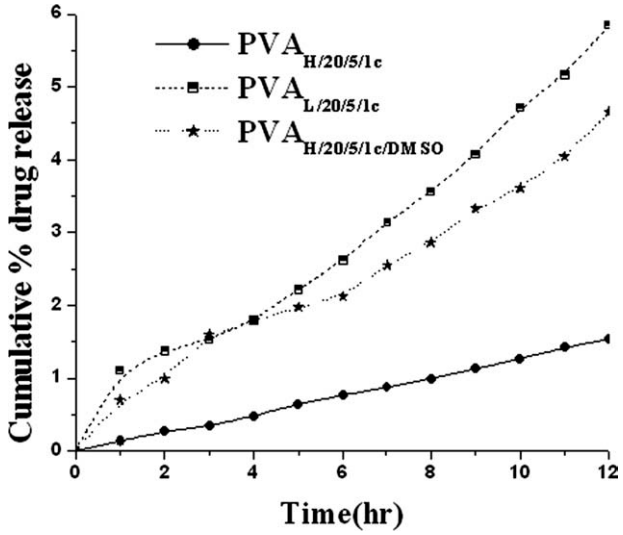

Figure 6 Cumulative percent drug (diltiazem hydrochloride) release study through various PVA hydrogel membranes.

$PVA_{L/20/5/1c}$ at the initial stage shows weak bursting effect compared to $PVA_{H/20/5/1c.DMSO}$, may be due to its high-water imbibing feature. It then slows down below $PVA_{H/20/5/1c/DMSO}$ and achieves a steady release rate. A crossover point has been noticed after 3 h release where both these membranes have identical elution rate. $PVA_{H/20/5/1c}$ shows super-slow release kinetics whereas other two hydrogels show appreciably faster release getting close to achieving steady drug concentration and thus have practical significance. Drug release profiles displayed in Figure 6 have interesting correlation with swelling behavior of these hydrogels. Samples such as $PVA_{H/20/5/1c/DMSO}$ and $PVA_{L/20/5/1c}$ show noticeably faster release rate despite of high percentage of postswell crystallinity. Additionally, they have deswelled comparatively slowly than $PVA_{H/20/5/1c.}$ It is, therefore, clear that elution of diltiazem hydrochloride from these hydrogel, is never been diffusion controlled but depends on molecular relaxation of PVA macrochains. This fact can be explained by two different reasons. First, the molecular weight of the drug is quite high and so its inherent resistance against diffusion is always active. Second, crystal domains of $PVA_{L/20/5/1c}$ and $PVA_{H/20/5/1c/DMSO}$ in swelled state act as local crosslinks and achieves elastomeric character previously demonstrated through tensile property analysis. The intercrosslink chain segments relax faster and allow more drugs to pass through when compared with $PVA_{H/20/5/1c.}$ The release rate was determined through fitting the data of Figure 6 into standard rate expressions, and it was found that it follows first-order kinetics. This means, faster release through $PVA_{L/20/5/1c}$ and $PVA_{H/20/5/1c/DMSO}$ eventually helps in achieving steady drug concentration of 180 mg in 24 h for an initial drug loading of 1.5 g. Alternatively, two or more hydrogel patches can be simultaneously used to match the cumulative drug requirement in the body for treatment.

CONCLUSIONS

PVA-based hydrogel membranes were prepared following freeze-thaw technique, and the gels were characterized. It was found that crystallinity development due to freeze-thaw operation could be traced by studying microstructure of the gels but due to higher equilibrium water retention, it was not detected through XRD analysis. Crystallinity clearly detected in some of the gels especially in PVA_H modified with PEG and DMSO and in PVA_L hydrogels—all treated for continuous 5 h, in the postswelled state due to dissolution of the amorphous portions in water. Swelled state crystallinity could also be visualized through AFM and PLM studies. Mechanical properties tested both in preswelled and postswelled states well complied with the gross morphology of the hydrogel membranes and proved to be interesting in this article. Hydrogels that showed superior physicomechanical properties were selected for *in vitro* controlled release of diltiazem hydrochloride. A steady release through skin to the blood (skin and blood replica were used) was observed for all the hydrogels tested; DMSO-modified PVA_H and PVA_L hydrogel membranes showed higher release with more practical significance while neat PVA_H showed super-slow release.

References

1. Finch, C. A. Poly(vinyl alcohol)-Properties and Application; Wiley: Bristol, Great Britain, 1973.
2. Matsuzawa, S.; Hondo, Y.; Kawauchi, Y.; Kawauchi, Y.; Kume, M.; Tanigami, T.; Ogasawara, K. Colloid Polym Sci 1987, 265, 810.
3. Xiao. C.; Zhou, G. Polym Degrad Stab 2003, 18, 297.
4. Bandyopadhyay, A.; De-Sarkar, M.; Bhowmick, A. K. J Mater Sci 2005, 40, 5233.
5. Bandyopadhyay, A.; De-Sarkar, M.; Bhowmick, A. K. J Polym Sci Part B: Polym Phys 2005, 43, 2399.
6. Bolto, B.; Tran, T.; Hoang, M.; Xie, Z. Prog Polym Sci 2009, 34, 969.
7. Krumova, M.; Lopez, D.; Benavente, R.; Mijangos, C. Polymer 2000, 41, 9265.
8. Gobben, B.; Vanderberg, H. W. A.; Burgeman, D.; Smolders, C. Polymer 1985, 26, 1737.
9. Yu, J.; Lee, C. H.; Hong, W. H. Chem Eng Process 2002, 41, 693.
10. Shibayama, M.; Sato, M.; Kimura, Y.; Fujiwara, H.; Nomura, S. Polymer 1998, 29, 336.
11. Doretti, L.; Ferrara, D.; Gattolin, P.; Lora, S. Talanta 1997, 44, 859.
12. Lee, K. Y.; Mooney, D. J. Chem Rev 2001, 101, 1869.
13. Seo, J-K.; Jung, J. L-H.; Kim, Mi-R.; Kim, J. B.; Nam, S-W.; Kim, S-K. Aqu Eng 2001, 24, 181.

14. Kim, S.; Kim, J. H.; Jeon, O.; Kwon, I. C.; Park, K. Eur J Pharm Biopharm 2009, 71, 420.
15. McGann, M. J. p; Higginbotham, C. L.; Geever, L. M.; Nugent, M. J. D. Int J Pharm 2009, 71, 420.
16. Juntanon, K.; Niamlang, S.; Rujiravanit, R.; Sirivat, A. Int J Pharm 2008, 356, 1.
17. Westedt, U.; Kalinowski, M.; Wittmar, M.; Merdan, T. J Controlled Release 2007, 119, 41.
18. Nugent, M. J. D.; Hanley, A.; Tomkins, P. T.; Higginbotham, C. L. J Mater Sci Mater Med 2005, 16, 1149.
19. Mari, Y.; Tokura, H.; Yoshikawa, M. J Mater Sci 1997, 32, 491.
20. Ricciardi, R.; Auriemma, F.; De-Rosa, C.; Lauprtre, F. Macromolecules 2004, 37, 1921.
21. Hassan, C. M.; Peppas, N. A. Adv Polym Sci 2000, 153, 38.
22. lozinsky, V. I.; Damshkalu, L. G.; Shaskol'skii, B. L.; Babushkina, T. A.; Kurochkim, B. L. Colloid J 2007, 69, 747.
23. Mansur, H. S.; Ore'fice, R. L.; Mansur, A. A. P. Polymer 2004, 45, 7193.
24. Awadhia, A.; Agaral, S. L. Solid State Ionics 2007, 178, 951.
25. Tacx, J. C. J. F.; Scholfellers, H. M.; Brands, A. G. M. Polymer 2000, 41, 947.
26. Suwantong, O.; Opanasopit, P.; Ruktanonchai, U.; Supaphol, P. Polymer 2007, 48, 7546.
27. Siddaramaiah; Kumar, P.; Divya, K.; Mhemavathi, B.; Manjula, D. J Macrom Sci Part A: Pure Appl Chem 2006, 43, 601.
28. Braun-Falco, O.; Korting, H. C. Hautarzt 1986, 37, 126.
29. Bodde, H. E.; Roemele, P. E.; Star, W. M. Photochem Photobiol 2002, 75, 418.
30. Lee, J.; Jin-Lee, K.; Jang, J. Polym Test 2008, 27, 360.
31. Muller-Plathe, F. Macromolecules 1998, 31, 6721.